
InSpaceType: Reconsider Space Type in Indoor Monocular Depth Estimation

Cho-Ying Wu¹ Quankai Gao¹ Chin-Cheng Hsu¹
Te-Lin Wu² Jing-Wen Chen¹ Ulrich Neumann¹

¹University of Southern California, ²University of California, Los Angeles
{choyingw, quankaig, chincheh, jchen885, uneumann}@usc.edu
{telinwu}@g.ucla.edu

Indoor monocular depth estimation has attracted increasing research interest. Most previous works have been focusing on methodology, primarily experimenting with NYU-Depth-V2 (NYUv2) Dataset, and only concentrated on the overall performance over the test set. However, little is known regarding robustness and generalization when it comes to applying monocular depth estimation methods to real-world scenarios where highly varying and diverse functional *space types* are present such as library or kitchen. A study for performance breakdown into space types is essential to realize a pretrained model’s performance variance. To facilitate our investigation for robustness and address limitations of previous works, we collect InSpaceType, a high-quality and high-resolution RGBD dataset for general indoor environments. We benchmark 12 recent methods on InSpaceType and find they severely suffer from performance imbalance concerning space types, which reveals their underlying bias. We extend our analysis to 4 other datasets, 3 mitigation approaches, and the ability to generalize to unseen space types. Our work marks the first in-depth investigation of performance imbalance across space types for indoor monocular depth estimation, drawing attention to potential safety concerns for model deployment without considering space types, and further shedding light on potential ways to improve robustness. See <https://depthcomputation.github.io/DepthPublic> for data and the supplementary document. The benchmark list on the GitHub project page keeps updates for the latest monocular depth estimation methods.

1 Introduction

Given an image input I , monocular depth estimation’s target is to predict pixel-level depth map D corresponding to I . It is a fundamental task in 3D vision for indoor applications, such as AR/VR gaming systems [38, 64, 56, 59, 57, 62, 61], robot assistance and navigation [15], 3D photo creation [51], and novel view synthesis [13]. Challenges for indoor scenes lie in addressing highly diverse environments and arbitrarily arranged objects cluttered in the near field. Especially performances optimized for one environment may not apply to another due to highly varying structures between different space types of indoor environments.

Most monocular depth estimation works begin from algorithmic perspectives, including advances in network architecture [31, 29, 8, 22, 72, 25, 6, 32, 44, 29, 60], loss function [5, 18, 69, 33], and learning paradigm on self-supervised learning [63, 21, 77, 71]. NYU-Depth-V2 (NYUv2) pioneers in collecting indoor dense depth and thereafter becomes useful for monocular depth estimation in indoor scenes.

While being prominent in many prior studies, using NYUv2 as the only primary indoor depth estimation benchmark can bring potential shortcomings: (1) They always report error or accuracy numbers on the whole test set and overlook the variance of performance across different indoor *space types*, which becomes a main concern in robustness when an edge-user applies pretrained models to uncommon or tailed space types and may observe degradation. Objects and textures are highly diverse for indoor scenes and may be specific to some spaces. For example, kitchenware is specific to kitchen and rarely appear in other spaces, or desk and chair are specific to the classroom. Therefore, when a training set misses some space types, performances easily drop due to unseen

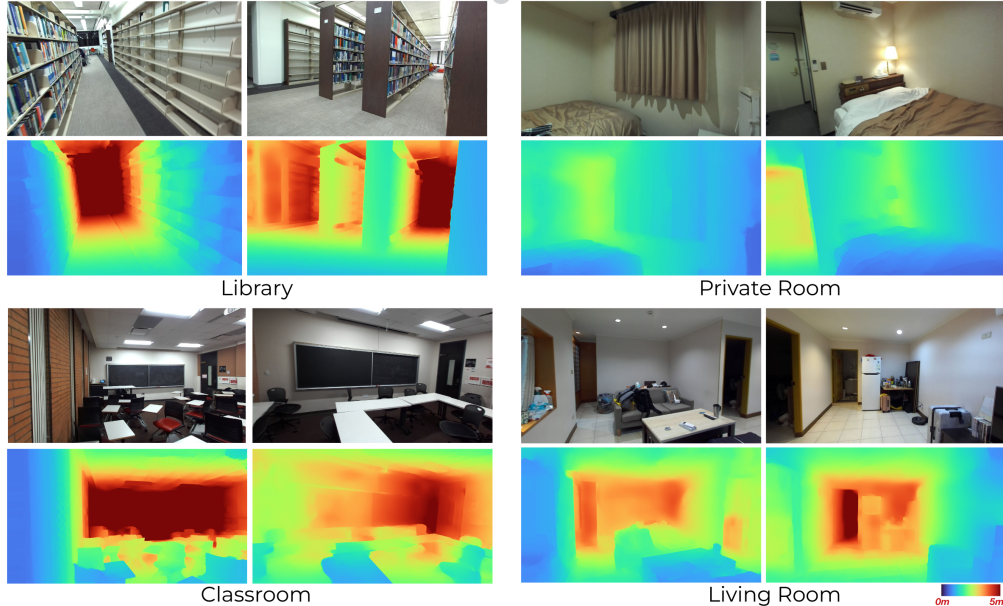


Figure 1: Data samples of our InSpaceType Dataset.

objects or arrangements specific to those types. This issue becomes more serious because private spaces appear more often than other spaces in NYUv2. Without a breakdown across space types, the **practicability** of prior methods is still *without verification*. (2) NYUv2 suffers from relatively low resolution (480×640), an older camera imaging model, and high noise levels. These downsides make evaluations on NYUv2 less reliable and meet the needs of real high-quality applications.

To enhance robustness and address the aforementioned problems, we take a deeper analysis of indoor space types using our novel dataset, *InSpaceType*, for *benchmark and evaluation*. InSpaceType is collected by an off-the-shelf modern stereo camera system [1] with a high resolution (1242×2208), much less noise, high-quality depth maps aligned with images, and optimized performance to near-range depth sensing that is suitable for indoor scenes. We compare with other commonly used evaluation protocols for indoor monocular depth estimation in Table 1. Fig. 1 show data examples.

InSpaceType captures common space types, including private room, office, hallway, lounge, meeting room, large room, classroom, library, kitchen, playroom, living room, and bathroom. A hierarchical system is designed to describe these indoor space types. As the first step, 12 high-performing methods pretrained on NYUv2 are collected for InSpaceType zero-shot benchmarks, including supervised and self-supervised learning methods. The overall performances and type breakdown are exhibited. We find that those prior methods suffer from severe performance imbalance between space types. They perform well in head types such as private room ($\delta_1 = 92.05$) but much worse in tailed types such as large room ($\delta_1 = 54.93$). The presented type breakdown is practical as it *goes beyond an average score and reveals performance variances on types*. Our analysis helps us understand strength and weakness of a pretrained model and potentially reveals its underlying biases.

In addition to NYUv2, 3 other training datasets, including SimSIN (aggregation of Replica [53], Matterport3D [11], and Habitat-Matterport3D), UniSIN [63], and Hypersim [48], are experimented. We dig into characteristics in performance trained on these datasets and enumerate certain space types these datasets tend to have bias towards or against. In particular, we find synthetic or simulation datasets cannot accurately capture the intricate complexities of cluttered or small objects in real scenes, which is common in spaces such as kitchen. To mitigate performance imbalance across types, 3 popular strategies are investigated: class re-weighting [12, 20], class-balanced sampling[24], and meta-learning[65, 58]. Dividing the studied 12 types into 3 groups based on their spatial functions and then examining the generalizability between groups, we find generalization to unseen types is challenging. The best δ_1 accuracy can be as high as 98.12 for intra-group evaluation but drops to 59.02 in the worst case of inter-group evaluation. Our findings reveal that generalization to unseen groups is challenging due to high diversity of objects and mismatched scales across types. Overall, this work serves a practical purpose for robustness and emphasizes the importance of the usually

Table 1: Comparison of popular evaluation protocols for indoor monocular depth estimation.

Dataset	Purpose	Resolution	Sensor	Real or Synthetic	RGB-Imaging Quality	Scene Diversity (# of scenes, # of RGBD pairs)
Diode [54]	Indoor + Outdoor	1024×768	Lidar	Real	High	Very Low (2 scenes, 753 indoor pairs)
IBims-1 [26]	Indoor focused	640×480	Lidar	Real	Good	Low (20 scenes, 100 pairs)
NYUv2 [52]	Indoor focused	640×480	Kinect-v1	Real	Noisy	Medium (private room focused, 654 pairs)
VA [63]	Indoor focused	640×640	-	Synthetic	High	Very Low (1 scene, 3523 pairs)
InSpaceType	Indoor focused	2208×1242	Stereo	Real	High	High (88 scenes, 1260 pairs)

overlooked factor- space type in indoor environments. We draw attention to potential safety concerns for model deployment without considering performance variance across space types.

Our contributions are summarized as follows:

- To our best knowledge, we are the first to present a thorough analysis that considers space type in indoor monocular depth estimation. We benchmark 12 recent methods and reveal that they are biased towards/against certain types. We emphasize the importance of being aware of such bias for real-world applications.
- We collect a dataset, InSpaceType, to facilitate our purpose of benchmarking and analyzing the variance of performances across multiple space types.
- We analyze 4 commonly-used training sets in indoor monocular depth estimation and enumerate their strengths and weaknesses towards certain space types. We further investigate 3 popular methods to mitigate performance imbalance.

2 Related Work

2.1 Indoor Monocular Depth Estimation

Monocular depth estimation is a fundamental task in computer vision. Very early methods find cues in similar regions, shades, or motion to assign depth values [14], or use probabilistic models for depth estimation [50]. This task has especially been popular during deep learning era. NYUv2 pioneers to collect a dense depth dataset for indoor scenes toward to goal.

Supervised method. Most methods operate in supervised learning and directly learn from paired RGBD data in the training set. Earlier deep methods include advances in architecture like fully convolutional neural network [27] or operating in different learning paradigms such as multi-task learning [16], transfer learning [3], dual-stream network [30, 75], or multi-scale network [39]. We organize more recent research directions as follows.

- Loss design and discretized depth intervals: DORN [18] uses a space-increasing discretization strategy and recasts the depth regression as ordinal regression. Adabins [5] designs adaptive discretization and combines pixel-level regression loss and bin-center density loss. LocalBins [6] learns per-pixel discretization instead of global distribution.
- Planarity: BTS [28] use multi-scale planar guidance to estimate depth. P3Depth [42] estimates plane coefficients for pieces and uses them for adaptive fusion.
- Conditional random fields (CRFs): Early probabilistic approaches build on CRFs [34, 47]. Recently NeWCRFs [72] applies CRFs in windows to reduce computation overhead in fully connected CRFs.
- Normal: Normal is helpful in depth regularization. VNL [69] enforces virtual normal constraints for depth prediction. IronDepth [4] uses normal map to propagate depth between pixels.
- Mixed-dataset training: MiDaS [46] pioneers to collect 12 different mixed data source and results in high generalization of depth estimation. DPT [45] further improves results using vision transformers. ZoeDepth [7] is based on DPT to further predict metric depth. LeReS [70, 41] also trains on mixed dataset for highly robust depth estimation. Depth-Anything [68] proposes to use semantics and better training strategies to attain very high robustness.
- Transformer: DepthFormer [31] and PixelFormer [2] both use vision transformers and large models for higher accuracy. GLPDepth [25] extracts global and local features with transformers and combines them with attention. Combined with transformers, MIM [66] studies masked image modeling and builds upon large transformer models [35] for visual pretraining to learn good representation first and then finetune on downstream tasks. AiP-T [40] uses VQGAN [17] and represents depth in a unified token space to attain high accuracy.

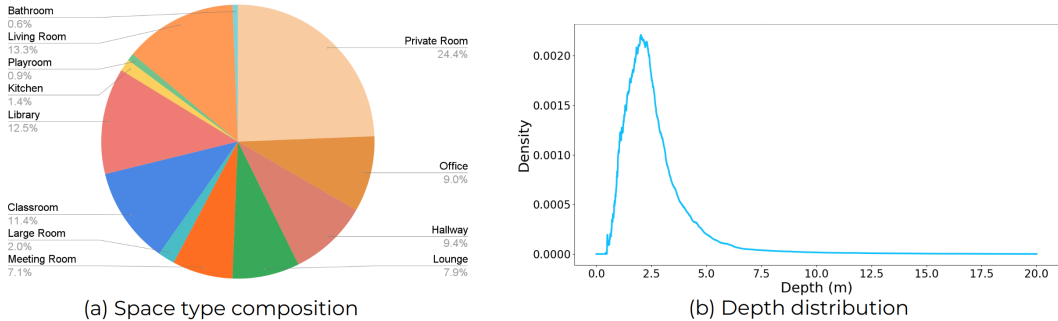


Figure 2: Statistics for InSpaceType evaluation set.

Self-Supervised method. Most methods use NYUv2 and learn from consecutive frames with photometric consistency [9, 74, 77]. DistDepth [63] adopts a distillation loss to learn from relative-depth pretrained models and incorporate left-right stereo consistency to learn metric depth.

2.2 Evaluation on Indoor Monocular Depth Estimation

Diode [54] collects both outdoor and indoor scenes. It collects high-quality data, but it contains very low diversity with only 2 scenes for evaluation. IBims-1 [26] is also limited in the amount of scenes. VA [63] renders complex and high-quality images and depth maps but is only limited to one scene. See Table 1 for the organization.

NYUv2 [52] is still popular in the evaluation of indoor monocular depth estimation. However, it is collected by an older Kinect-v1 system [73] with noisy depth measurements and noisy imaging for RGB patterns. Its resolution is only 640×480 , which is much smaller than the needs of recent applications for robotics or high-resolution synthesis. Besides, NYUv2 mainly focuses on smaller and private rooms to evaluate performance. To overcome these limitations, our InSpaceType adopts a recent high-quality integrated stereo camera [1] to collect high-resolution images and depth. InSpaceType covers general-purpose and highly diverse indoor scenes, including private household spaces, workspaces, and campus scenes. We design a hierarchical system to describe space types and benchmark recent high-performing methods with detailed performance breakdown. This breakdown helps gain better understanding of performance variance across different spaces.

3 InSpaceType Dataset

We capture images and depth maps computed from left-right stereo pairs using a high-quality integrated stereo camera system, Zed-2i [1]. Its baseline is 12cm, field of view (FOV) is 120° , working distance is up to 20m, and its backend engine enables dense depth outputs

It is particularly optimized for ranges within 15m, whose average error is within 5% from its specification. This matches our needs to work in indoor environments. We operate in its ULTRA mode to output a high resolution of 2208×1242 . The stereo camera device is anchored on a hand-held stabilizer during data collection. Wide FOV makes scene images contain more cues to estimate distance. We do not zoom into small objects or flat walls, which will cause ambiguity in the scene scale. The pitch angle is about within $\pm 30^\circ$, and the roll angle is within $\pm 10^\circ$. This setting enriches scenes captured from different viewing directions without resulting in strange scenes or reaching a threshold where excessively large angles would eliminate cues that indicate depth ranges. For better quality, we also avoid non-Lambertian areas such as mirrors or highly reflective surfaces.

Our environments cover household spaces, workspaces, and campus spaces, including private room, office, hallway, lounge, meeting room, large room, classroom, library, kitchen. 88 different environments are visited in total. We record at 15fps while walking around those spaces. Around 40K images are collected. To create the evaluation set, we manually select 1260 images from all the environments.

Our selection criteria include (1) clear imaging with minimal motion blur, (2) not selecting from nearby 10 frames, and (3) containing sufficient cues that hint depth scales of the scene. Fig. 2 shows the dataset statistics. See Supplementary for more dataset descriptions.

Table 2: **InSpaceType benchmark: overall performance.** The best number is in bold, and the second-best is underlined. We include ten recent high-performing methods, including supervised and self-supervising learning paradigms.

Method	Year	Architecture	MAE	AbsRel	SqRel	RMSE	δ_1	δ_2	δ_3
Supervised Learning									
BTS [28]	arXiv'19	DenseNet-161	0.3602	0.1445	0.1162	0.5222	81.65	95.57	98.54
AdaBins [5]	CVPR'21	Unet+AdaBins	0.3341	0.1333	0.0957	0.4922	83.64	96.36	98.92
DPT [45]	ICCV'21	DPT-Hybrid	0.3090	<u>0.1224</u>	0.0773	0.4616	85.96	97.17	<u>99.19</u>
GLPDepth [25]	arXiv'22	Mit-b4	0.3068	0.1239	0.0788	0.4527	86.05	97.36	99.16
IronDepth [4]	BMVC'22	EfficientNet-B5	0.3271	0.1276	0.1022	0.4894	85.30	<u>96.37</u>	98.84
Decomposition [23]	ECCV'22	EfficientNet-B5	0.3274	0.1278	0.1025	0.4899	85.25	96.35	98.83
NeWCRFs [72]	CVPR'22	Swin-Large	0.3028	0.1251	0.0823	0.4541	86.04	96.68	98.94
PixelFormer [2]	WACV'23	Swin-Large	<u>0.2982</u>	0.1225	<u>0.0761</u>	<u>0.4392</u>	<u>86.08</u>	97.03	99.10
MIM [67]	CVPR'23	SwinV2-Large	0.2807	0.1100	0.0679	0.4244	88.58	97.59	99.28
ZoeDepth (NK) [7]	arXiv'23	BeiT-Large	0.2469	0.0969	0.0527	0.3834	90.76	98.19	99.50
ZoeDepth (N) [7]	arXiv'23	BeiT-Large	0.2484	0.0956	0.0528	0.3887	90.81	98.22	99.52
DepthAnything [68]	arXiv'24	ViT-L	0.2397	0.0928	0.0506	0.3806	90.01	98.09	99.54
Self-Supervised Learning									
DistDepth (DPT-Hybrid) [63]	CVPR'22	ResNet152	0.4688	0.1746	0.1718	0.6877	74.71	94.18	98.60
DistDepth (DPT-Large) [63]	CVPR'22	ResNet152	0.3817	0.1447	0.1094	0.5758	81.05	95.46	98.69

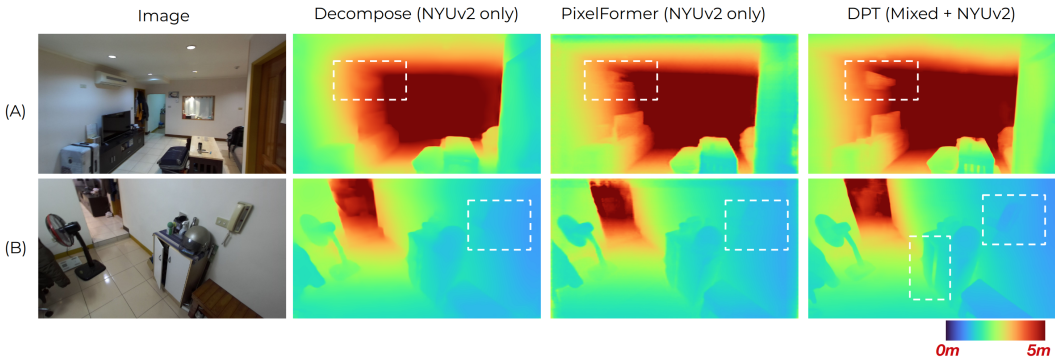


Figure 3: **Regions that trained on NYUv2 only cannot show.** InSpaceType contains several object arrangements that NYUv2 does not include, such as wall-hanging air-conditioner and phone are mostly exclusive to Asian styles rooms; a tilted viewing direction for pitch angle is shown in (B), where training on NYUv2 only cannot give robust results because NYUv2 has minor viewing pitch angle changes. DPT in their setting trains on 10 different dataset + NYUv2 (mixed-set training) attains more pleasant results. To verify generalizability, InSpaceType serves as a testbed to help find out cases where training on popular NYUv2 only cannot show.

4 Cross-Dataset Benchmarks

[I: Benchmarks] As the first step, we collect recent 11 high-performing methods and fetch open-sourced models pretrained on NYUv2 and use them to make inferences on InSpaceType. The following methods are included: DPT [45], GLPDepth [25], AdaBins [5], PixelFormer [2], NeWCRFs [72], BTS [28], MIM [67], IronDepth [4], Decomposition [23], ZoeDepth [7], Depth-Anything [68]¹. We adopt error (AbsRel, SqRel, RMSE) and accuracy metrics (δ_1 , δ_2 , δ_3 with base factor 1.25) commonly used in the literature of monocular depth estimation for evaluation. To compensate for different camera intrinsics between NYUv2 and InSpaceType, we follow prior protocols for cross-dataset evaluation [37, 65] and use median-scaling to calibrate prediction and groundtruth scale.

Table 2 shows the results. For reference, the performance for these methods on NYUv2 benchmark (in terms of lower RMSE) is listed: Depth-Anything > ZoeDepth > MIM > PixelFormer > NeWCRFs > GLPDepth > IronDepth > Decomposition > DPT > AdaBins > BTS. The ranking on InSpaceType is consistent to NYUv2. Depth-Anything, ZoeDepth, MIM and PixelFormer are top among published methods. They use large-size transformers, showing large models can learn better representations. We also notice DPT surpasses other methods in some metrics. This is because DPT was first pretrained on a mixture of datasets and then finetuned on NYUv2. Larger amount of data involved during pretraining helps the model to learn better representations for generalization. To verify the generalizability in Fig. 3, we show examples where training only on NYUv2 may stumble.

¹We use NYUv2 fine-tuned indoor model for evaluation. See https://github.com/DepthComputation/InSpaceType_Benchmark for full space type breakdown

Table 3: **Performance breakdown by space types.** We study MIM and PixelFormer, which are top-performing published methods. Beside the breakdown, we also list top-5 space types based on lower/higher error (RMSE) and accuracy (δ_1). Easy and hard type are listed based on co-occurrence.

Type	MIM Results						PixelFormer Results					
	AbsRel	SqRel	RMSE	δ_1	δ_2	δ_3	AbsRel	SqRel	RMSE	δ_1	δ_2	δ_3
Private room	0.0927	0.0342	0.2556	92.05	98.99	99.83	0.1013	0.0372	0.2638	90.17	98.70	99.80
Office	0.1106	0.0532	0.3313	87.67	97.42	99.44	0.1271	0.0649	0.3658	84.60	96.38	99.19
Hallway	0.1229	0.0805	0.5463	85.66	96.52	98.89	0.1418	0.0880	0.5236	81.46	96.40	99.05
Lounge	0.1316	0.1290	0.7447	84.15	96.22	98.93	0.1500	0.1624	0.8215	79.92	94.79	98.41
Meeting room	0.0984	0.0483	0.3636	91.70	98.69	99.64	0.1103	0.0551	0.3873	88.25	98.57	99.76
Large room	0.2683	0.4499	1.3915	54.93	83.89	93.91	0.2125	0.3119	1.1396	67.71	88.59	95.40
Classroom	0.0781	0.0334	0.3071	94.52	99.25	99.83	0.0912	0.0403	0.3368	91.37	99.14	99.86
Library	0.1342	0.0978	0.6281	85.61	96.57	98.57	0.1530	0.1242	0.6527	82.57	94.88	97.73
Kitchen	0.1482	0.0791	0.3374	82.31	95.42	98.32	0.1819	0.0978	0.3521	78.86	93.05	96.63
Playroom	0.0702	0.0276	0.2466	94.54	98.25	99.79	0.1010	0.0476	0.3042	92.11	97.23	99.15
Living room	0.1033	0.0502	0.3448	89.07	97.88	99.52	0.1132	0.0568	0.3601	87.35	97.31	99.34
Bathroom	0.1456	0.0772	0.2788	83.45	96.07	98.13	0.1439	0.0570	0.2488	83.72	96.55	98.36

	MIM	PixelFormer
Top-5 Lower RMSE	playroom, private room, bathroom, classroom, office	bathroom, private room, playroom, classroom, kitchen
Top-5 Higher δ_1	playroom, classroom, private room, meeting room, living room	playroom, private room, classroom, meeting room, living room
Easy type	playroom, private room, classroom	playroom, private room, classroom
Top-5 Higher RMSE	large room, lounge, library, hallway, meeting room	large room, lounge, library, hallway, meeting room
Top-5 Lower δ_1	large room, kitchen, bathroom, lounge, library	large room, kitchen, lounge, hallway, library
Hard type	large room, lounge, library	large room, lounge, library, hallway

Self-supervised direction attracted more attention due to no depth groundtruth involved during training but generally lower performance, especially in driving scenarios. Indoor self-supervised methods received less attention due to the lack of indoor stereo pairs to enable robust monocular depth scales. DistDepth [63] pioneers to create synthetic indoor stereo data and enable more stable scale estimation from monocular images and becomes current SOTA. We adopt DistDepth to show the current performance gap between supervised/ self-supervised learning. The gap tells us how far it is between training with/ without depth groundtruth.

[II: Breakdown by Space Type] Then, we break down MIM and PixelFormer’s performances by space types and show results in Table 3. We show performance on each space type, list out top-5 high/ low-performing types, and show easy/ hard types based on the concordance in lower error/ higher accuracy (easy) and the opposite (hard). The easy types for MIM and PixelFormer are the same: playroom, private room, and classroom; the common hard types are: large room, lounge, and library. Clear easy and hard types indicate that strength and weakness for these models are apparent, showing they are biased towards/against some specific types. The easy and hard types are highly overlapping for both MIM and PixelFormer, which further unveils potential bias underlying NYUv2’s training data. The most frequent space type for NYUv2 is private room and living room, which are typically small spaces. By contrast, large spaces of farther ranges are those less capable of.

From the above analysis, we find performance varies a lot across different space types. The identification of easy and hard types provides insights into the suitability of using pretrained models in specific scenarios or the need to avoid them. Furthermore, this analysis highlights that the learned representations from NYUv2 still have a gap to transfer to other space types. See Supplementary for performance breakdown for other methods and hierarchical description for types.

[III: More Training Dataset Generalization] Next, we validate performances trained on other popular training datasets. Specifically, we include the following datasets and models: SimSIN [63](self-supervised by DistDepth, ResNet152 [19]), UniSIN [63] (self-supervised by DistDepth, ResNet152), Hypersim [48] (supervised, ConvNeXt-Base [36]). SimSIN and UniSIN datasets are recently introduced along with DistDepth [63] with pretrained models released on both. Both datasets mainly serve the purpose of self-supervised studies that recently become popular. Thus, we consider including such self-supervised oriented datasets, SimSIN and UniSIN, and use DistDepth pretrained model for analysis. Table 4 and 5 show the results. We show depth distribution of these datasets in Supplementary for reference.

- SimSIN: It contains data from Replica [53], Matterport3D [11], and HM3D [43], which are also focused on household spaces. From Table 4, its easy types are private room and living room, and hard types are large room, classroom, meeting room, and lounge. Its strength and weakness are also obvious, showing that SimSIN is heavily biased towards household spaces, and is especially under-performing in workspaces or campus scenes.
- UniSIN: From Table 4, its easy types are bathroom and hallway, and hard type is only large room. One can observe UniSIN has less bias towards space types, having only few easy and hard types. We assume it is because UniSIN collects data from more diverse environments and avoids clear bias.

Table 4: **Performance trained on SimSIN and UniSIN.** We leverage pretrained $\text{DistDepth}_{(\text{DPT-Large})}$ -ResNet152 models [63] in both cases.

Type	Trained on SimSIN						Trained on UniSIN					
	AbsRel	SqRel	RMSE	δ_1	δ_2	δ_3	AbsRel	SqRel	RMSE	δ_1	δ_2	δ_3
Private room	0.1509	0.0986	0.4447	79.36	96.48	99.53	0.1738	0.1102	0.4539	72.81	93.65	98.68
Office	0.1812	0.1606	0.5789	74.01	93.47	97.80	0.1656	0.1113	0.5020	75.04	94.86	98.98
Hallway	0.1597	0.1239	0.6324	78.12	94.92	98.64	0.1262	0.0765	0.4977	84.79	96.91	99.37
Lounge	0.1841	0.2148	0.9037	73.86	93.11	97.94	0.1380	0.1428	0.7351	82.41	96.77	98.95
Meeting room	0.1962	0.2491	0.9417	66.91	93.58	99.45	0.1300	0.1104	0.5937	83.94	97.36	99.63
Large room	0.1842	0.2619	1.0727	72.79	91.87	97.88	0.1608	0.2112	0.9447	75.95	94.83	98.68
Classroom	0.2069	0.3288	1.0292	67.11	91.66	98.51	0.1313	0.1166	0.6077	84.12	97.96	99.74
Library	0.1857	0.1913	0.8307	75.14	93.11	97.44	0.1230	0.1146	0.6958	85.61	96.48	98.91
Kitchen	0.2524	0.2083	0.5649	59.22	87.44	96.12	0.2741	0.1997	0.5740	52.30	85.15	96.28
Playroom	0.1597	0.1147	0.5946	75.59	97.95	99.67	0.1486	0.0822	0.4755	78.63	98.23	99.84
Living room	0.1600	0.1166	0.5284	77.05	94.90	98.89	0.1644	0.1153	0.5106	76.37	93.66	98.48
Bathroom	0.1751	0.1153	0.3900	74.22	94.07	98.46	0.1384	0.0409	0.2168	84.67	95.28	99.68
All	0.1746	0.1719	0.6877	74.72	94.18	98.61	0.1509	0.1143	0.5602	78.96	95.38	98.97

	SimSIN	UniSIN
Top-5 Lower RMSE	bathroom, private room, living room, kitchen, office	bathroom, private room, playroom, hallway, office
Top-5 Higher δ_1	private room, hallway, living room, playroom, library	library, hallway, bathroom, classroom, meeting room
Easy type	living room, private room	bathroom, hallway
Top-5 Higher RMSE	large room, classroom, meeting room, lounge, library	large room, lounge, library, classroom, meeting room
Top-5 Lower δ_1	kitchen, meeting room, classroom, large room, lounge	kitchen, private room, office, large room, living room
Hard type	large room, classroom, meeting room, lounge	large room

Table 5: **Performance trained on Hypersim.** We adopt supervised learning with standard L_2 loss on a ConvNeXt backbone [36].

Type	Hypersim					
	AbsRel	SqRel	RMSE	δ_1	δ_2	δ_3
Private room	0.1321	0.0607	0.3376	84.55	97.26	99.36
Office	0.1678	0.1085	0.4916	76.01	93.60	97.87
Hallway	0.2126	0.1912	0.8347	65.67	89.89	97.15
Lounge	0.1937	0.2254	0.9403	71.31	92.58	97.58
Meeting room	0.1315	0.0837	0.5333	81.49	98.23	99.74
Large room	0.2525	0.4125	1.3897	56.48	85.13	94.95
Classroom	0.1258	0.0740	0.4700	85.07	98.50	99.80
Library	0.1766	0.1664	0.8654	73.53	93.54	98.03
Kitchen	0.2417	0.1343	0.4347	62.81	90.25	96.43
Playroom	0.1629	0.1132	0.5663	77.09	93.87	99.15
Living room	0.1485	0.0872	0.4519	80.91	95.40	98.95
Bathroom	0.1648	0.0627	0.2908	76.11	95.80	98.89
All	0.1592	0.1187	0.5803	77.95	94.99	98.60

	Hypersim
Top-5 Lower RMSE	bathroom, private room, kitchen, living room, classroom
Top-5 Higher δ_1	classroom, private room, meeting room, living room, playroom
Easy type	private room, living room, classroom
Top-5 Higher RMSE	large room, lounge, library, hallway, playroom
Top-5 Lower δ_1	large room, kitchen, hallway, lounge, library
Hard type	large room, library, hallway, lounge

- **Hypersim:** From Table 5, its easy types are private room, classroom, living room, and its hard types are large room, library, hallway, and lounge. It also has obvious bias, especially bias towards household spaces and classroom and bias against large room or types missed in the dataset such as library or hallway. Though Hypersim contains high-quality renderings from synthetic environments, it also focuses on household spaces and biases against several common space types.

One can find SimSIN and Hypersim, both are rendered from simulation platforms, have more obvious bias types, compared with UniSIN of real-world data collection. This indicates current trends to curate indoor synthetic data focus more on head types, especially private room and living room as the most frequent application scenarios, and may miss tailed types such as library, lounge, or hallway that is common but easily overlooked. Deploying models trained on those datasets may not be robustness in the wild. We point out this observation to call for attention when curating synthetic datasets.

- **Special Type:** We find kitchen is a special type, which is of lower RMSE but also very low accuracy score δ_1 in SimSIN and Hypersim. We assume this is because kitchen contains many cluttered small objects, such as bottles, kitchenware, and utensils in the near field. SimSIN uses Habitat simulator [49], which renders images from synthetic (Replica [53]) or scanned but incomplete mesh (Matterport3D [11] and HM3D [43]). Hypersim is pure synthetically rendered from delicately modeled spaces. Those simulation strategies cannot faithfully reflect high complexity of cluttered and small objects in real scenes. Therefore, they attain lower δ_1 , which indicates how object shapes are correctly estimated in the depth domain. This serves as an understanding of simulation versus real data, showing a gap still exists to transfer knowledge well to real scenes.

The above studies consider InSpaceType as a testing set. To further validate InSpaceType, we further create a training set for InSpaceType. The training set includes all 40K images except 1260 evaluation images and their nearby 2 frames. We experiment with training on InSpaceType, NYUv2 [52], and

Table 6: **Zero-Shot generalization.** Hypersim, NYUv2, and InSpaceType are adopted as training sets. Replica (Left Table) and VA (Right Table) are used as indoor testing sets. Training on InSpaceType induces better results to validate InSpaceType’s quality for zero-shot cross-dataset scenarios.

Test on Replica	AbsRel	RMSE	δ_1	δ_2	δ_3	Test on VA	AbsRel	RMSE	δ_1	δ_2	δ_3
Hypersim	0.1547	0.3833	79.88	92.94	97.39	Hypersim	0.1620	0.2997	77.65	94.53	98.29
NYUv2	0.1524	0.3652	80.62	93.11	97.65	NYUv2	0.1584	0.2650	80.19	95.21	98.78
InSpaceType	0.1441	0.3347	81.82	93.51	98.12	InSpaceType	0.1507	0.2483	81.74	95.50	99.01

Table 7: **Results of training and evaluation on train/eval splits of InSpaceType.**

	Private room	Office	Hallway	Lounge	Meeting room	Large room
RMSE	0.1344	0.1729	0.2354	0.3185	0.1778	0.3153
δ_1	98.41	96.93	95.81	96.88	98.11	98.22
	Classroom	Library	Kitchen	Playroom	Living room	Bathroom
RMSE	0.1725	0.2543	0.1825	0.1707	0.1556	0.0943
δ_1	98.77	97.34	94.63	96.86	98.14	96.57

Table 8: **Comparison for imbalance mitigation strategies.** Class weights (CR), class-balanced sampling (CBS), and meta-learning (ML) are examined. Type standard deviation (t-STD) of RMSE and δ_1 computes standard deviation on twelve types. Higher t-STD indicates higher performance variation or more imbalance across types.

Model	Strategy	AbsRel	SqRel	RMSE	δ_1	δ_2	δ_3	t-STD _{RMSE}	t-STD _{δ_1}
Conv-sml	w/o	0.0542	0.0181	0.1918	97.66	99.60	99.88	0.0642	1.4850
Conv-sml	w/ CR	0.0606	0.0202	0.2071	97.06	99.52	99.86	0.0630	1.4371
Conv-sml	w/ CBS	0.0501	0.0166	0.1816	98.04	99.66	99.90	0.0600	1.1632
Conv-sml	w/ ML	0.0482	0.0160	0.1769	98.21	99.68	99.89	0.0580	1.3829
Conv-b	w/o	0.0510	0.0174	0.1846	97.96	99.63	99.89	0.0673	1.2236
Conv-b	w/ CR	0.0567	0.0196	0.1986	97.47	99.58	99.87	0.0619	1.1577
Conv-b	w/ CBS	0.0439	0.0146	0.1667	98.52	99.73	99.90	0.0561	1.0990
Conv-b	w/ ML	0.0451	0.0156	0.1692	98.44	99.70	99.90	0.0540	1.1269

Hypersim [48] using DPT-Hybrid (initialized from pretrained weights) and test on Replica [10] and VA [63]. Results in Table 6 show better zero-shot cross-dataset generalization for the introduced InSpaceType.

5 Intra-Dataset Study

In Section 4, we emphasize cross-dataset benchmarks with space types. We benchmark several high-performing methods with a breakdown into space types. Further, we unveil and enumerate potential bias in several training sets. Next, we focus on InSpaceType itself for deeper analysis.

[IV: Dataset Fitting] We use InSpaceType training set and train on small-size ConvNeXt network using standard L_2 loss supervised by groundtruth depth and test on the evaluation set. We use ConvNeXt networks for their high performance and as general-purpose networks to investigate data fitting and bias mitigation without loss of generality. Results in Table 7 show most space types can fit in well when training on all types together. Large room and lounge are large-size spaces and naturally result in slightly higher RMSE. Kitchen’s δ_1 is a bit lower than other types due to the reason specified in [III]. It is worth noting that there is an apparent trend: for errors, larger rooms and longer ranges tend to have a higher estimation error; for accuracy, arbitrarily arranged small objects in the near field are challenging, a frequent scenario for kitchen.

[V: Mitigation of Uneven Distribution] We also experiment with several basic and popular strategies to help mitigate the imbalance issue across different types. Specifically, we examine class re-weighting (CR) [12, 20], class-balanced sampling (CBS) [24], and Reptile-like meta-learning (ML) [65]. CR use weights inversely proportional to occurrences to compensate for types of higher occurrences. CBS is to sample from all classes with equal probability. Reptile ML uses bi-level optimization for learning to learn across tasks to attain higher generalizability and may mitigate unbalance. We adopt ConvNeXt-small (Conv-sml) and ConvNeXt-base (Conv-b) as backbones and experiment on InSpaceType train and evaluation set. From Table 8, one can find CBS and ML are better strategies to attain lower standard deviation across types (t-STD) and better overall performance. Though CR attains lower t-STD, its overall performance drop as well. This is because CR could harm head-class performances as observed in literature [55, 76].

[VI: Generalization to Unseen Types] In addition to generalization to unseen datasets, we are also curious about generalization to unseen types. We next divide the whole InSpaceType training

Table 9: **Performance for training and evaluating on different groups.** $G1 \rightarrow$ specifies the training group (G), and the entries below are evaluation groups. Three depth ranges: close, medium, and far are used to evaluate performances on scenes of different scales. See the text for the definition.

$G1 \rightarrow$ Type	AbsRel	SqRel	RMSE	δ_1	δ_2	δ_3	$G1 \rightarrow$ Range	AbsRel	SqRel	RMSE	δ_1	δ_2	δ_3
G1	0.0511	0.0134	0.1461	98.12	99.71	99.92	Close	0.0984	0.0476	0.2877	89.48	98.08	99.66
G2	0.1607	0.1092	0.5501	77.22	94.91	98.90	Medium	0.1376	0.1241	0.5935	80.47	94.59	98.37
G3	0.2669	0.3851	1.1987	59.02	85.02	94.12	Far	0.2897	0.4375	1.3003	55.57	82.74	93.16
$G2 \rightarrow$ Type	AbsRel	SqRel	RMSE	δ_1	δ_2	δ_3	$G2 \rightarrow$ Range	AbsRel	SqRel	RMSE	δ_1	δ_2	δ_3
G1	0.1418	0.0666	0.3497	82.29	96.81	99.39	Close	0.1063	0.0464	0.2720	87.97	97.80	99.59
G2	0.0673	0.0244	0.2250	96.33	99.45	99.86	Medium	0.1169	0.0728	0.4263	87.27	97.75	99.34
G3	0.2139	0.2485	0.9424	68.38	90.35	96.61	Far	0.2336	0.2886	1.0028	66.01	88.76	95.90
$G3 \rightarrow$ Type	AbsRel	SqRel	RMSE	δ_1	δ_2	δ_3	$G3 \rightarrow$ Range	AbsRel	SqRel	RMSE	δ_1	δ_2	δ_3
G1	0.1902	0.1416	0.4776	71.95	93.10	98.09	Close	0.2184	0.2070	0.5838	66.78	90.83	97.38
G2	0.1967	0.1657	0.6116	69.16	92.38	98.04	Medium	0.2129	0.2243	0.7016	68.46	89.54	96.39
G3	0.0727	0.0395	0.3473	95.79	99.14	99.71	Far	0.0819	0.0491	0.3784	94.08	98.65	99.50

set into different splits, train on each division, and then evaluate on InSpaceType eval split. The whole training set is divided into three groups (G) based on types. G1: private room, kitchen, living room, bathroom; G2: office, hallway, meeting room, classroom; G3: lounge, large room, playroom, library. G1 is for household spaces; G2 is related to work or studies; G3 contains longer-range spaces. Models have only seen data from their respective group at training. For instance, a model trained on G1 cannot access RGBD pairs of classroom or hallway during training. The categorization is based on similarity between types and concerns a situation where one collects training data almost in the same functionality that matches the primary application scenarios without considering different user scenarios. This is frequently encountered in scope-focused applications. Such as gaming VR systems are primarily for households, but the performance may drop with outlier use cases in classroom or workplace. Results in Table 9 left half show generalization to other types, and the right half shows evaluation on different depth ranges. Three depth ranges are defined: close, medium, and far. Close: a scene whose maximal depth is approximately within 5 meters. Medium: a scene whose maximal depth is approximately within 5-10 meters. Far: a scene whose maximal depth is approximately within 10-20 meters. The average maximal depth value is 3.78m for G1, 5.49m for G2, and 12.08m for G3. We present another training set categorization based on ranges in Supplementary.

Training on specific groups can produce good performance on its dedicated types. However, one can observe training on only some types encounters severe issues in generalization to other unseen types, which further exhibit high variation between different indoor environments, and pretrained knowledge on some types may not easily transfer to other types. For example, training on G1’s household spaces cannot generalize to large or spacious room ($G1 \rightarrow G3$ or Far) and show higher RMSE and lower δ_1 . Most indoor training datasets, such as NYUv2 or simulation from Matterport3D or Replica, are mostly curated for household spaces or smaller rooms. This may serve the needs of applications mainly for private room, but it potentially poses a training set bias towards close-range estimation, and the models trained on these datasets cannot be deployed to address different scenarios. Besides, we also observe training on large or spacious spaces (G3) can attain a bit better generalization to smaller rooms than the reverse setting, comparing between $G3 \rightarrow G1$ and $G1 \rightarrow G3$ or between $G3 \rightarrow$ Close and $G1 \rightarrow$ Far. We visualize the cross-group generalization result in Fig. 4.

6 Conclusion

Unlike previous methods that focus on algorithmic developments, we are the first work to consider space types in indoor monocular depth estimation for robustness and practicability in deployment. We point out limitations in previous evaluations where performance variances across types are overlooked and present a novel dataset, InSpaceType, along with a hierarchical space type definition to facilitate our study. We give thorough studies to analyze and benchmark performance based on space types. Ten high-performing methods are examined, and we find they suffer from severe performance imbalance between space types. We analyze a total of 4 training datasets and enumerate their strength and weakness space types. 3 popular strategies, namely, class reweighting, type-balanced sampler, and meta-learning, are studied to mitigate imbalance. Further, we find generalization to unseen space types challenging due to high diversity of objects and mismatched scales across types. Overall, this work pursues a practical purpose and emphasizes the importance of this usually overlooked factor-space type in indoor environments. We call for attention to safety concerns for model deployment without considering performance variance across space types.

Limitations. This work only considers monocular depth estimation. Other popular scopes for depth estimation such as outdoor domain, stereo approaches, or multiview scene reconstruction may also

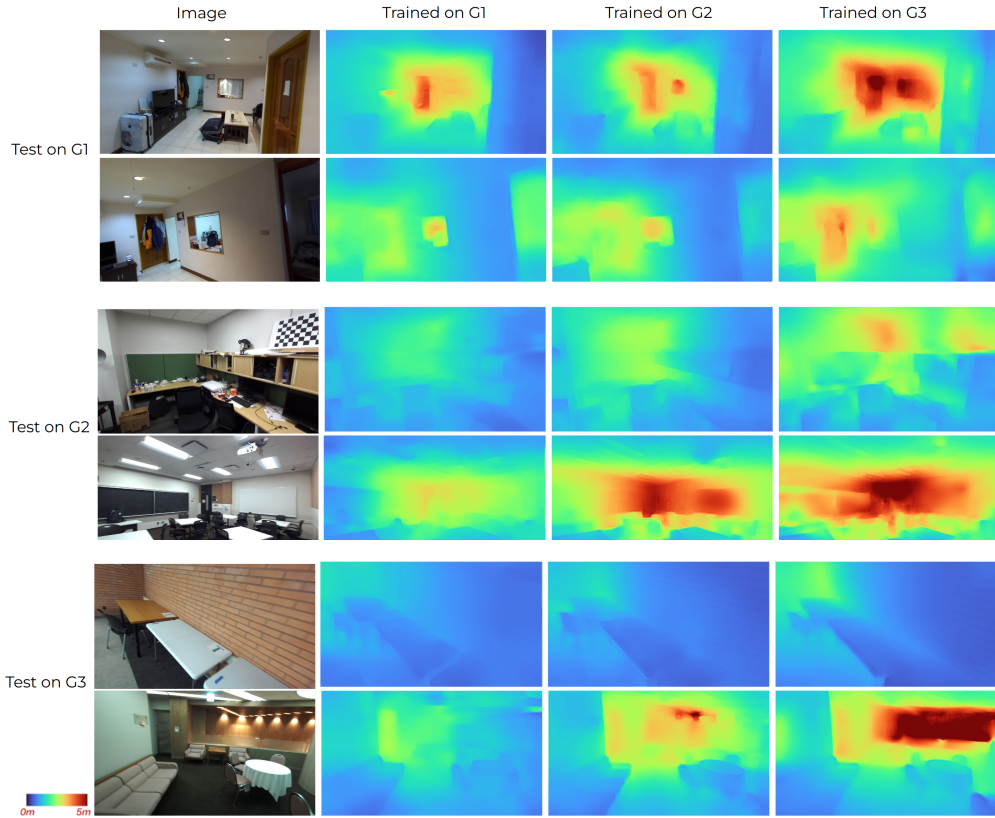


Figure 4: Visualization of cross-group generalization.

suffer from performance imbalance across different types. We choose to operate on monocular depth estimation since it is the most fundamental task with only an image needed and is especially widely useful in many recent popular applications or deployed systems such as indoor AR on smartphones, VR gaming, novel view synthesis, or video generation for indoor scenes. This work specifically zooms into the factor space type, but this may not be the only important factor blocking the generalization.

References

- [1] Zed2i-stereolabs. <https://www.stereolabs.com/zed-2i/>.
- [2] Ashutosh Agarwal and Chetan Arora. Attention attention everywhere: Monocular depth prediction with skip attention. In *WACV*, 2023.
- [3] Ibraheem Alhashim and Peter Wonka. High quality monocular depth estimation via transfer learning. *arXiv preprint arXiv:1812.11941*, 2018.
- [4] Gwangbin Bae, Ignas Budvytis, and Roberto Cipolla. Irondepth: Iterative refinement of single-view depth using surface normal and its uncertainty. *BMVC*, 2022.
- [5] Shariq Farooq Bhat, Ibraheem Alhashim, and Peter Wonka. Adabins: Depth estimation using adaptive bins. In *CVPR*, 2021.
- [6] Shariq Farooq Bhat, Ibraheem Alhashim, and Peter Wonka. Localbins: Improving depth estimation by learning local distributions. In *ECCV*, 2022.
- [7] Shariq Farooq Bhat, Reiner Birkel, Diana Wofk, Peter Wonka, and Matthias Müller. Zoedepth: Zero-shot transfer by combining relative and metric depth. *arXiv preprint arXiv:2302.12288*, 2023.
- [8] Jia-Wang Bian, Huangying Zhan, Naiyan Wang, Tat-Jun Chin, Chunhua Shen, and Ian Reid. Auto-rectify network for unsupervised indoor depth estimation. *TPAMI*, 2021.
- [9] Jia-Wang Bian, Huangying Zhan, Naiyan Wang, Zhichao Li, Le Zhang, Chunhua Shen, Ming-Ming Cheng, and Ian Reid. Unsupervised scale-consistent depth learning from video. *IJCV*, 2021.
- [10] Rohan Chabra, Julian Straub, Christopher Sweeney, Richard Newcombe, and Henry Fuchs. Stereodnet: Dilated residual stereonet. In *CVPR*, 2019.
- [11] Angel Chang, Angela Dai, Thomas Funkhouser, Maciej Halber, Matthias Niebner, Manolis Savva, Shuran Song, Andy Zeng, and Yinda Zhang. Matterport3D: Learning from RGB-D data in indoor environments. In *3DV*, 2017.

- [12] Yin Cui, Menglin Jia, Tsung-Yi Lin, Yang Song, and Serge Belongie. Class-balanced loss based on effective number of samples. In *CVPR*, 2019.
- [13] Kangle Deng, Andrew Liu, Jun-Yan Zhu, and Deva Ramanan. Depth-supervised nerf: Fewer views and faster training for free. In *CVPR*, 2022.
- [14] Mariella Dimiccoli. Monocular depth estimation for image segmentation and filtering. *Dept. Signal Theory Commun., Ph. D. dissertation, Univ. Politecnica de Catalunya, Barcelona, Spain*, 2009.
- [15] Xingshuai Dong, Matthew A Garratt, Sreenatha G Anavatti, and Hussein A Abbass. Towards real-time monocular depth estimation for robotics: A survey. *IEEE Transactions on Intelligent Transportation Systems*, 2022.
- [16] David Eigen and Rob Fergus. Predicting depth, surface normals and semantic labels with a common multi-scale convolutional architecture. In *ICCV*, 2015.
- [17] Patrick Esser, Robin Rombach, and Bjorn Ommer. Taming transformers for high-resolution image synthesis. In *CVPR*, 2021.
- [18] Huan Fu, Mingming Gong, Chaohui Wang, Kayhan Batmanghelich, and Dacheng Tao. Deep ordinal regression network for monocular depth estimation. In *CVPR*, 2018.
- [19] Kaiming He, Xiangyu Zhang, Shaoqing Ren, and Jian Sun. Deep residual learning for image recognition. In *CVPR*, 2016.
- [20] Chen Huang, Yining Li, Chen Change Loy, and Xiaoou Tang. Learning deep representation for imbalanced classification. In *CVPR*, 2016.
- [21] Pan Ji, Runze Li, Bir Bhanu, and Yi Xu. Monoindoor: Towards good practice of self-supervised monocular depth estimation for indoor environments. In *ICCV*, 2021.
- [22] Hualie Jiang, Laiyan Ding, Junjie Hu, and Rui Huang. Plnet: Plane and line priors for unsupervised indoor depth estimation. In *3DV*, 2021.
- [23] Jinyoung Jun, Jae-Han Lee, Chul Lee, and Chang-Su Kim. Depth map decomposition for monocular depth estimation. In *ECCV*, 2022.
- [24] Bingyi Kang, Saining Xie, Marcus Rohrbach, Zhicheng Yan, Albert Gordo, Jiashi Feng, and Yannis Kalantidis. Decoupling representation and classifier for long-tailed recognition. In *ICLR*, 2020.
- [25] Doyeon Kim, Woonghyun Ga, Pyunghwan Ahn, Donggyu Joo, Sehwan Chun, and Junmo Kim. Global-local path networks for monocular depth estimation with vertical cutdepth. *arXiv:2201.07436*, 2022.
- [26] Tobias Koch, Lukas Liebel, Friedrich Fraundorfer, and Marco Korner. Evaluation of cnn-based single-image depth estimation methods. In *ECCVW*, 2018.
- [27] Iro Laina, Christian Rupprecht, Vasileios Belagiannis, Federico Tombari, and Nassir Navab. Deeper depth prediction with fully convolutional residual networks. In *3DV*, 2016.
- [28] Jin Han Lee, Myung-Kyu Han, Dong Wook Ko, and Il Hong Suh. From big to small: Multi-scale local planar guidance for monocular depth estimation. *arXiv preprint arXiv:1907.10326*, 2019.
- [29] Boying Li, Yuan Huang, Zeyu Liu, Danping Zou, and Wenxian Yu. Structdepth: Leveraging the structural regularities for self-supervised indoor depth estimation. In *ICCV*, 2021.
- [30] Jun Li, Reinhard Klein, and Angela Yao. A two-streamed network for estimating fine-scaled depth maps from single rgb images. In *CVPR*, 2017.
- [31] Zhenyu Li, Zehui Chen, Xianming Liu, and Junjun Jiang. Depthformer: Exploiting long-range correlation and local information for accurate monocular depth estimation. *arXiv preprint arXiv:2203.14211*, 2022.
- [32] Zhenyu Li, Xuyang Wang, Xianming Liu, and Junjun Jiang. Binsformer: Revisiting adaptive bins for monocular depth estimation. *arXiv preprint arXiv:2204.00987*, 2022.
- [33] Ce Liu, Suryansh Kumar, Shuhang Gu, Radu Timofte, and Luc Van Gool. Va-depthnet: A variational approach to single image depth prediction. In *ICLR*, 2023.
- [34] Fayao Liu, Chunhua Shen, and Guosheng Lin. Deep convolutional neural fields for depth estimation from a single image. In *CVPR*, 2015.
- [35] Ze Liu, Han Hu, Yutong Lin, Zhuliang Yao, Zhenda Xie, Yixuan Wei, Jia Ning, Yue Cao, Zheng Zhang, Li Dong, et al. Swin transformer v2: Scaling up capacity and resolution. In *CVPR*, 2022.
- [36] Zhuang Liu, Hanzi Mao, Chao-Yuan Wu, Christoph Feichtenhofer, Trevor Darrell, and Saining Xie. A convnet for the 2020s. *CVPR*, 2022.
- [37] Xuan Luo, Jia-Bin Huang, Richard Szeliski, Kevin Matzen, and Johannes Kopf. Consistent video depth estimation. *ACM Transactions on Graphics (TOG)*, 2020.
- [38] Wolfgang Meringer, Markus Wirth, Daniel Roth, Georg Michelson, and Bjoern M Eskofier. Stereopsis only: Validation of a monocular depth cues reduced gamified virtual reality with reaction time measurement. *IEEE Transactions on Visualization and Computer Graphics*, 2022.
- [39] Michel Moukari, Sylvaine Picard, Loïc Simon, and Frédéric Jurie. Deep multi-scale architectures for monocular depth estimation. In *ICIP*, pages 2940–2944, 2018.
- [40] Jia Ning, Chen Li, Zheng Zhang, Zigang Geng, Qi Dai, Kun He, and Han Hu. All in tokens: Unifying output space of visual tasks via soft token. *arXiv preprint arXiv:2301.02229*, 2023.
- [41] Nikolay Patakin, Anna Vorontsova, Mikhail Artemyev, and Anton Konushin. Single-stage 3d geometry-preserving depth estimation model training on dataset mixtures with uncalibrated stereo data. In *CVPR*, 2022.

- [42] Vaishakh Patil, Christos Sakaridis, Alexander Liniger, and Luc Van Gool. P3Depth: Monocular depth estimation with a piecewise planarity prior. In *CVPR*, 2022.
- [43] Santhosh K Ramakrishnan, Aaron Gokaslan, Erik Wijmans, Oleksandr Maksymets, Alex Clegg, John Turner, Eric Undersander, Wojciech Galuba, Andrew Westbury, Angel X Chang, et al. Habitat-matterport 3D dataset (HM3D): 1000 large-scale 3D environments for embodied AI. *NeurIPS Datasets and Benchmarks Track*, 2021.
- [44] Michael Ramamonjisoa, Michael Firman, Jamie Watson, Vincent Lepetit, and Daniyar Turmukhambetov. Single image depth prediction with wavelet decomposition. In *CVPR*, 2021.
- [45] René Ranftl, Alexey Bochkovskiy, and Vladlen Koltun. Vision transformers for dense prediction. *ICCV*, 2021.
- [46] René Ranftl, Katrin Lasinger, David Hafner, Konrad Schindler, and Vladlen Koltun. Towards robust monocular depth estimation: Mixing datasets for zero-shot cross-dataset transfer. *TPAMI*, 2020.
- [47] Elisa Ricci, Wanli Ouyang, Xiaogang Wang, Nicu Sebe, et al. Monocular depth estimation using multi-scale continuous crfs as sequential deep networks. *TPAMI*, 2018.
- [48] Mike Roberts, Jason Ramapuram, Anurag Ranjan, Atulit Kumar, Miguel Angel Bautista, Nathan Paczan, Russ Webb, and Joshua M Susskind. Hypersim: A photorealistic synthetic dataset for holistic indoor scene understanding. In *ICCV*, 2021.
- [49] Manolis Savva, Abhishek Kadian, Oleksandr Maksymets, Yili Zhao, Erik Wijmans, Bhavana Jain, Julian Straub, Jia Liu, Vladlen Koltun, Jitendra Malik, et al. Habitat: A platform for embodied ai research. In *CVPR*, 2019.
- [50] Ashutosh Saxena, Sung Chung, and Andrew Ng. Learning depth from single monocular images. *NIPS*, 2005.
- [51] Meng-Li Shih, Shih-Yang Su, Johannes Kopf, and Jia-Bin Huang. 3D photography using context-aware layered depth inpainting. In *CVPR*, 2020.
- [52] Nathan Silberman, Derek Hoiem, Pushmeet Kohli, and Rob Fergus. Indoor segmentation and support inference from rgbd images. In *ECCV*, 2012.
- [53] Julian Straub, Thomas Whelan, Lingni Ma, Yufan Chen, Erik Wijmans, Simon Green, Jakob J Engel, Raul Mur-Artal, Carl Ren, Shobhit Verma, et al. The replica dataset: A digital replica of indoor spaces. *arXiv preprint arXiv:1906.05797*, 2019.
- [54] Igor Vasiljevic, Nick Kolkin, Shanyi Zhang, Ruotian Luo, Haochen Wang, Falcon Z Dai, Andrea F Daniele, Mohammadreza Mostajabi, Steven Basart, Matthew R Walter, et al. Diode: A dense indoor and outdoor depth dataset. *arXiv preprint arXiv:1908.00463*, 2019.
- [55] Hongxin Wei, Lue Tao, Renchunzi Xie, Lei Feng, and Bo An. Open-sampling: Exploring out-of-distribution data for re-balancing long-tailed datasets. In *ICML*, 2022.
- [56] Cho-Ying Wu and Jian-Jiun Ding. Occlusion pattern-based dictionary for robust face recognition. In *ICME*, 2016.
- [57] Cho Ying Wu and Jian Jiun Ding. Occluded face recognition using low-rank regression with generalized gradient direction. *Pattern Recognition*, 80:256–268, 2018.
- [58] Cho-Ying Wu and Jian-Jiun Ding. Nonconvex approach for sparse and low-rank constrained models with dual momentum. *arXiv preprint arXiv:1906.02433*, 2019.
- [59] Cho-Ying Wu, Chin-Cheng Hsu, and Ulrich Neumann. Cross-modal perceptionist: Can face geometry be gleaned from voices? In *CVPR*, 2022.
- [60] Cho-Ying Wu, Xiaoyan Hu, Michael Happold, Qiangeng Xu, and Ulrich Neumann. Geometry-aware instance segmentation with disparity maps. *arXiv preprint arXiv:2006.07802*, 2020.
- [61] Cho-Ying Wu and Ulrich Neumann. Salient building outline enhancement and extraction using iterative l0 smoothing and line enhancing. In *2019 IEEE International Conference on Image Processing (ICIP)*, 2019.
- [62] Cho-Ying Wu and Ulrich Neumann. Scene completeness-aware lidar depth completion for driving scenario. In *ICASSP*, 2021.
- [63] Cho-Ying Wu, Jialiang Wang, Michael Hall, Ulrich Neumann, and Shuochen Su. Toward practical monocular indoor depth estimation. In *CVPR*, 2022.
- [64] Cho-Ying Wu, Qiangeng Xu, and Ulrich Neumann. Synergy between 3dmm and 3d landmarks for accurate 3d facial geometry. In *3DV*, 2021.
- [65] Cho-Ying Wu, Yiqi Zhong, Junying Wang, and Ulrich Neumann. Meta-optimization for higher model generalizability in single-image depth prediction. *arXiv preprint arXiv:2305.07269*, 2023.
- [66] Zhenda Xie, Zigang Geng, Jingcheng Hu, Zheng Zhang, Han Hu, and Yue Cao. Revealing the dark secrets of masked image modeling. In *CVPR*, 2023.
- [67] Zhenda Xie, Zigang Geng, Jingcheng Hu, Zheng Zhang, Han Hu, and Yue Cao. Revealing the dark secrets of masked image modeling. *CVPR*, 2023.
- [68] Lihe Yang, Bingyi Kang, Zilong Huang, Xiaogang Xu, Jiashi Feng, and Hengshuang Zhao. Depth anything: Unleashing the power of large-scale unlabeled data. *arXiv preprint arXiv:2401.10891*, 2024.
- [69] Wei Yin, Yifan Liu, Chunhua Shen, and Youliang Yan. Enforcing geometric constraints of virtual normal for depth prediction. In *ICCV*, 2019.

- [70] Wei Yin, Jianming Zhang, Oliver Wang, Simon Niklaus, Long Mai, Simon Chen, and Chunhua Shen. Learning to recover 3d scene shape from a single image. In *CVPR*, 2021.
- [71] Zehao Yu, Lei Jin, and Shenghua Gao. P²net: Patch-match and plane-regularization for unsupervised indoor depth estimation. In *ECCV*, 2020.
- [72] Weihao Yuan, Xiaodong Gu, Zuo Zhuo Dai, Siyu Zhu, and Ping Tan. New crfs: Neural window fully-connected crfs for monocular depth estimation. *CVPR*, 2022.
- [73] Zhengyou Zhang. Microsoft kinect sensor and its effect. *IEEE multimedia*, 2012.
- [74] Wang Zhao, Shaohui Liu, Yezhi Shu, and Yong-Jin Liu. Towards better generalization: Joint depth-pose learning without posenet. In *CVPR*, 2020.
- [75] Yiqi Zhong, Cho-Ying Wu, Suya You, and Ulrich Neumann. Deep rgb-d canonical correlation analysis for sparse depth completion. *NeurIPS*, 2019.
- [76] Boyan Zhou, Quan Cui, Xiu-Shen Wei, and Zhao-Min Chen. Bbn: Bilateral-branch network with cumulative learning for long-tailed visual recognition. In *CVPR*, 2020.
- [77] Junsheng Zhou, Yuwang Wang, Kaihuai Qin, and Wenjun Zeng. Moving indoor: Unsupervised video depth learning in challenging environments. In *CVPR*, 2019.